Published in final edited form as:
Life Sci. 2010 March 13; 86(11-12): 448–454. doi:10.1016/j.lfs.2010.01.017.

Nitric oxide synthase activation and oxidative stress, but not intracellular zinc dyshomeostasis, regulate ultraviolet B light-induced apoptosis

Lei Wang[a,b], **Wei Liu**[a,b,c], **Suzanne H. Parker**[b], and **Shiyong Wu**[a,b,c,*]

[a]Department of Chemistry and Biochemistry, Ohio University, Athens, Ohio 45701

[b]Edison Biotechnology Institute, Ohio University, Athens, Ohio 45701

[c]Molecular and Cellular Biology Program, Ohio University, Athens, Ohio 45701

Abstract

Aims—To investigate the role of nitric oxide synthase and intracellular free zinc ion (Zn^{2+}) in regulation of ultraviolet B light (UVB)-induced cell damage and apoptosis.

Main methods—Real time confocal microscopy measurement was used to determine the changes of intracellular free zinc concentration under different conditions. Cell apoptotic death was determined using fluorescein isothiocyanate (FITC) conjugated-annexin V (ANX5)/PI labeling followed by flow cytometry. Western analysis was used to determine cell apoptosis and eNOS uncoupling.

Key findings—UVB induced an elevation of Zn^{2+} within 2 min of exposure. The UVB-induced intracellular Zn^{2+} elevation was dependent on the increase of constitutive nitric oxide synthase (cNOS) activity and production of superoxide. Removal of Zn^{2+} with a lower concentration (<25 μM) of N,N,N',N'-tetrakis (2-pyridylmethyl) ethylenediamine (TPEN), a Zn^{2+}-specific chelator, did not induce cell death or prevent cells from UVB-induced apoptosis. However, a higher [TPEN] (> 50 μM) was cytotoxic to cells, but prevented cells from further UVB-induced apoptosis. The higher [TPEN] also induced cNOS uncoupling. Furthermore, treating the cells with a membrane permeable superoxide dismutase (PEG-SOD) inhibited Zn^{2+} release and reduced apoptotic cell death after UVB treatment. The results demonstrated a complex and dynamic regulation of UVB-induced cell damage.

Significance—Our findings not only advance our understanding of the correlations between cNOS activation and Zn elevation, but also elucidated the role of cNOS in regulation of oxidative stress and apoptosis upon UVB-irradiation.

Keywords

Ultraviolet B light (UVB); nitric oxide synthase (NOS); nitric oxide ($NO^{\bullet}$); peroxynitrite ($ONOO^{-}$); oxidative stress; superoxide ($O_2^{\bullet-}$); zinc (Zn^{2+}) dyshomeostasis; apoptosis

Published by Elsevier Inc.

*Address correspondence to: Dr. Shiyong Wu, Edison Biotechnology Institute, 101 Konneker Laboratories, The Ridges, Building 25, Athens, OH 45701, Tel. (740) 597-1318, Fax (740) 593-4795; wus1@ohio.edu.

Introduction

The elevation of nitric oxide ($NO^{\bullet}$) in skin cells after ultraviolet light B (UVB) irradiation plays an important role in regulation of apoptosis (Lee et al. 2000; Yamaoka et al. 2004). In keratinocytes, $NO^{\bullet}$ is produced by constitutive nitric oxide synthase (cNOS), which is activated immediately by UVB-induced calcium flux (Deliconstantinos et al. 1996a; Lu et al. 2009). UVB also induces the production of superoxide ($O_2^{\bullet -}$) (Aitken et al. 2007; Deliconstantinos et al. 1996b), which could rapidly react with $NO^{\bullet}$ to form peroxynitrite ($ONOO^-$) (Beckman and Koppenol 1996; Groves 1999). Our recent study indicated that UVB-induced imbalance of $NO^{\bullet}/ONOO^-$ promotes apoptotic cell death (Wu et al. 2010). A higher level of $ONOO^-$ could also induce cNOS uncoupling by oxidizing the Zn^{2+}-thiolate-complex and releasing Zn^{2+} from the enzyme (Aravindakumar et al. 1999; Zou et al. 2002).

An elevation of intracellular Zn^{2+} ($[Zn^{2+}]_i$) has been shown to correlate to $NO^{\bullet}$ production and oxidative-stress-induced apoptosis (Bernal et al. 2008; Suh et al. 2008). Zinc is the second most highly abundant transition metal found in the human body and is released from zinc-binding proteins under oxidative stress. Zn^{2+} is essential for DNA and protein synthesis and the maintenance of DNA and RNA (Vallee and Falchuk 1993). Skin contains twenty percent of total body zinc. Maintaining zinc homeostasis is important in regulation of skin health. A chelation of zinc promotes apoptosis of keratinocytes and supplement of zinc protects skin from UV-induced DNA fragmentation and apoptosis (Leccia et al. 1999; McGowan et al. 1994; Parat et al. 1997). However, the physiological relationships among $NO^{\bullet}$ production, $[Zn^{2+}]_i$ elevation and apoptosis upon UVB-irradiation are not clear. In the present study, we show that UVB-irradiation induced a quick elevation of $[Zn^{2+}]_i$, which was dependent on the increase of cNOS activity and production of $O_2^{\bullet -}$. We also provide evidence that $[Zn^{2+}]_i$ elevation was not a cause of apoptosis, but Zn^{2+} dyshomeostasis could lead to uncoupling of cNOS. The increased amount of uncoupled cNOS results in an imbalance of $NO^{\bullet}/ONOO^-$, which promotes apoptosis of UVB-irradiated keratinocytes.

Materials and Methods

Cell culture

The immortalized human keratinocyte cell line HaCaT was kindly provided by Dr. Hongtao Yu (Jackson State University, MS) and cultured as a monolayer in DMEM (Cellgro) with 10% FBS (Cellgro) at 37°C with 5% CO_2. Human umbilical vein endothelial (HUVEC) cells were cultured in MCDB-131 medium (VEC Technologies) with 10% FBS (Cellgro) at 37°C with 5% CO_2.

Analysis of intracellular zinc concentration ($[Zn^{2+}]_i$)

For Real-time measurement, the cells were seeded in 35 mm plates one day before analysis. The cells were treated with N^G-monomethyl-L-Arginine (LNMMA, 100 μM, Sigma) for 2 h, N-Acetyl-L-Cysteine (LNAC, 25 mM, Sigma) for 2 h, TPEN (50 μM, Molecular Probes) for 15 min or PEG-SOD (100 unit/mL, Sigma) for 1 h before stained with NG-DCF (10 μM, N7991, Invitrogen) in the dark for 30 min. The NG-DCF dye was removed and cells were washed twice with phosphate buffered saline (PBS). The cells were then covered with PBS (400 μL) and UVB (50 mJ/cm^2) irradiated. The fluorescent images were acquired from 60 sec before to 600 sec after UVB-irradiation by a camera connected to a confocal microscope (LSM 510, Carl Zeiss) at the speed of 1 frame/5 sec at excitation and emission wavelengths of 506 nm and 531 nm, respectively.

For quantitative analysis of $[Zn^{2+}]_i$, the cells were seeded in 12-well tissue culture plates, treated with LNMMA, LNAC or TPEN and stained with NG-DCF as described above.

Immediately after irradiation, the buffer was replaced with 1 mL of fresh medium and TPEN was added to the designated wells. Fluorescence intensities were recorded immediately and 30 min after UVB-irradiation at wavelengths of 506/531 nm, respectively, using a Spectramax M2 plate reader (Molecular Devices).

Determination of cell apoptosis by flow cytometry

The cells were treated with SOD for 1 h before or TPEN for 15 min before and after UVB irradiation. At 24 h post-irradiation, the cells were harvested by 0.01% trypsin digestion and combined with the cells floating in the medium. The apoptotic cell death was analyzed by determination of the loss of membrane phospholipid symmetry and membrane integrity (Schindl et al. 1998; Vermes et al. 1995) using a fluorescein isothiocyanate (FITC) conjugated-annexin V (ANX5)/PI apoptosis detection kit (BD Biosciences) following the manufacturer's protocol. The ANX5/PI double-stained cells were analyzed by using a FACSort Flow Cytometer (Becton Dickinson) equipped with CellQuest software (Becton Dickinson). The parameters of the measurement were set at SSC 350; FL1 700; FL2 700, and a total 10,000 cells were counted.

Western blot analysis of PARP cleavage and eNOS uncoupling

The cells were treated with different concentration of TPEN for 15 min before and after UVB irradiation. The cells were lysed at 4°C in NP-40 lysis buffer (2% NP-40, 80 mM NaCl, 100 mM Tris-HCl, 0.1% SDS) containing a Proteinase Inhibitor Cocktail (Complete™, Roche Molecular Biochemicals) 24 h after UVB. The protein samples were then added to five-fold Laemmli buffer and boiled. These samples were separated on SDS-PAGE gel and then transferred onto a nitrocellulose membrane. The membrane was blocked with 5% (w/v) skim milk in Tris-Buffered Saline Tween-20 (TBST) for 1 h and then incubated with anti-poly (ADP-ribose) polymerase (anti-PARP) antibodies (Cell Signaling) at 4°C overnight. After washed with TBST, the membrane was incubated with HRP–conjugated anti-rabbit antibody for 1 h at room temperature. Membrane was then washed three times in TBST and two times in TBS, and developed in West Pico Supersignal Chemiluminescent substrate (Pierce).

To determine the SDS-resistant eNOS dimers and monomers, low-temperature SDS-PAGE under reducing conditions were performed as described before (Zou et al. 2002). The cells were treated with TPEN and harvested at the time points as indicated. The proteins were mixed with five-fold Laemmli buffer without boiling, electrophorezed on a reducing SDS-PAGE (with 2.5% 2-mercaptoethanol) at 4°C and then transferred onto a nitrocellulose membrane. The eNOS was detected by western blot analysis as described above. The intensities of the bands of coupled eNOS (eNOSc) and uncoupled eNOS (eNOSu) were quantitated using ImageJ (v1.42k, NIH).

UV Irradiation

UVB was generated from a 15 W UVB lamp (UVP), which has an emission spectra from 280–370 nm with a peak at 310 nm. The intensity of UVB was standardized by a UVB meter (UVP) and set at 3 mW/cm^2. The medium was replaced with PBS during the irradiation. After UV irradiation, fresh medium was added to each plate.

Statistical Analysis

Student's *t-test*was used to analyze the significance of data. $p<0.05$ was considered significant.

Results

UVB triggers $[Zn^{2+}]_i$ elevation in keratinocytes

Our recent studies indicate that UVB induced rapid increase of cNOS activity, which generated an imbalance of $NO^{\bullet}/ONOO^{-}$ and promoted apoptotic and skin damage (Wu et al. 2010). Since previous studies suggested that an alternation of $Zn^{2+}]_i$ was associated with $NO^{\bullet}$-induced neuronal cell death (Bossy-Wetzel et al. 2004; Cuajungco and Lees 1997), we determined whether $[Zn^{2+}]_i$ also plays a role in UVB-induced and $NO^{\bullet}$-mediated skin cell apoptosis. We first performed real-time measurement of $[Zn^{2+}]_i$ in HaCaT cells using an inverted laser-scanning confocal microscope. Intracellular free zinc was labeled with a zinc specific fluorescence dye - Newport Green-DCF (NG-DCF) and the fluorescence intensity was recorded by a camera connected to the confocal microscope at the speed of 1 frame/5 sec. Our data shows that while $[Zn^{2+}]_i$ remained the same in control cells (Fig. 1C), $[Zn^{2+}]_i$ started to increase in 2 min and peaked in 3 min after UVB-irradiation (Fig. 1A, 1B and 1D). The UVB-induced fluorescence was inhibited by a zinc specific chelator N,N,N',N'-tetrakis (2-pyridylmethyl) ethylenediamine (TPEN, Fig. 1E), which suggests that the increase of fluorescence is $[Zn^{2+}]_i$-dependent. Since $NO^{\bullet}$ peaked in 40 s post-UVB (Wu et al. 2010), our results indicate that Zn^{2+} homeostasis is alternated after $NO^{\bullet}$ elevation in skin cells upon UVB-irradiation.

A combination of NOS activation and oxidative stress leads to $[Zn^{2+}]_i$ elevation upon UVB

Our recent study indicates that UVB induced an immediate release of $O_2^{\bullet-}$, which rapidly reacts with $NO^{\bullet}$ to form $ONOO^{-}$ (Wu et al. 2010). To determine the contribution of $NO^{\bullet}$ and $O_2^{\bullet-}$ to UVB-induced elevation of $[Zn^{2+}]_i$, we assessed the extent of the effect of NOS inhibitor and antioxidant on $[Zn^{2+}]_i$ upon UVB-irradiation. An N-substituted L-Arg analog LNMMA was used to inhibit NOS activity and the glutathione (GSH) synthesis precursor LNAC was used to reduce oxidative stress. Our data shows that pre-treating the cells with LNMMA or LNAC inhibited UVB-induced elevation of $[Zn^{2+}]_i$ (Fig. 1F and 1G). These results suggest that $[Zn^{2+}]_i$ elevation is caused by a combination effect of NOS activation and oxidative stress upon UVB-irradiation. As an important signaling molecule to regulate diverse physiological events, $NO^{\bullet}$ is also produced by eNOS in endothelia HUVEC cells and regulates vascular remodeling and cell survival. The amount of $NO^{\bullet}$ release from HUVECs depends on various stimuli, such as UV irradiation and shear stress (Di Pietro et al. 2006). To determine whether UVB-induced and NOS/oxidative stress-mediated elevation of $[Zn^{2+}]_i$ is cell type independent, we analyzed the $[Zn^{2+}]_i$ elevation in HUVEC cells in the presence of LNMMA and LNAC under the same conditions as above. The $[Zn^{2+}]_i$ was quantitatively measured by a fluorescence plate reader at the indicated time points. The data shows that the $[Zn^{2+}]_i$ was rapidly increased 2.33±0.12 folds in HUVEC cells after exposure to UVB-irradiation (Fig. 2). The increased $[Zn^{2+}]_i$ was slowly decreased to 1.88±0.39 folds at 30 min post-irradiation. The UVB-irradiated cells that received TPEN (50 μM) did not fluoresce above the level of control cells or cells that had been treated with TPEN alone (Fig. 2). The UVB-induced increase of $[Zn^{2+}]_i$ was again inhibited by pre-treating the cells with LNMMA or LNAC (Fig. 2). The similar results were also observed using MEF and MCF-7 cells (data not shown). These results indicate that rapid elevation of $[Zn^{2+}]_i$ induced by UVB-irradiation is not cell-type specific.

Complex roles of Zn^{2+} in regulation of apoptosis without or with UVB-irradiation

An increase of $[Zn^{2+}]_i$ has been shown to be associated with apoptotic death of cells under various stimuli (Aizenman et al. 2000; Canzoniero et al. 1999; Lobner et al. 2000). However, free Zn^{2+} could also directly or indirectly protect cells from oxidative stress-induced apoptosis (Ha et al. 2006; Powell 2000; Taylor et al. 1997). To determine the role of released intracellular Zn^{2+} in UVB-induced apoptosis of keratinocytes, we determined apoptosis of HaCaT cells, which were treated with various concentrations of TPEN before and after UVB-irradiation.

Our data show that UVB-irradiation induced apoptosis was not affected by TPEN at a concentration below 25 μM (Fig. 3A). However, while higher concentrations of TPEN (50 μM and 75 μM) induced apoptosis by themselves, they also inhibited further apoptotic death induced by UVB (Fig. 3A). The results were further confirmed by determination of the extent of effects of high/low [TPEN] on UVB-induced poly (ADP-ribose) polymerase (PARP) cleavage, evidence widely used for detecting cells undergoing apoptosis. Treated cells by UVB caused cleavage of 116-kDa PARP to an 89-kDa fragment which is the marker for cell apoptosis. Neither low concentration (12.5 μM) nor high concentration (75 μM) of TPEN protects keratinocytes from PARP cleavage upon UVB irradiation (Fig. 3B).

To determine whether the concentration-dependent effect of TPEN on UVB-induced apoptosis correlates with the inhibition of cytosolic Zn^{2+} release, we analyzed $[Zn^{2+}]_i$ after treating the cells with different concentration of TPEN before UVB-irradiation. Our data shows that TPEN prevented UVB-induced $[Zn^{2+}]_i$ elevation even at 12.5 μM (Fig. 3C), a concentration of TPEN that had no effect on UVB-induced apoptosis (Fig. 3A). These results indicate that cytosolic free Zn^{2+} release did not cause apoptosis directly after UVB-irradiation. However, since high [TPEN] induced apoptosis and meanwhile protected cells from further apoptosis induced by UVB (Fig. 3A and 3B), our results also suggest that intracellular Zn^{2+} homeostasis plays a critical role in regulation of apoptosis without or with UVB-irradiation.

UVB induced production of $ONOO^-$ mediates $[Zn^{2+}]_i$ elevation and promotes apoptosis

Since inhibition of NOS activation eliminated UVB-induced free Zn^{2+} release (Fig. 1F), we investigated the mechanism of $NO^\bullet$-mediated alternation of intracellular Zn^{2+} homeostasis upon UVB-irradiation. Previous studies indicated that $NO^\bullet$ reacts quickly with $O_2^{\bullet-}$ to form $ONOO^-$ (Beckman and Koppenol 1996;Groves 1999), which has been shown to oxidize the zinc-thiolate complex and zinc-fingers of zinc-binding proteins including cNOS and result in the release of zinc from the complex (Aravindakumar et al. 1999;Pacher et al. 2007;Zou et al. 2002). Our recent study demonstrated that $ONOO^-$ was released in HaCaT cells almost immediately after UVB-irradiation (Wu et al. 2010). To determine whether UVB-induced $ONOO^-$ production leads to $[Zn^{2+}]_i$ elevation, we treated the cells with a membrane permeable polyethylene glycol modified superoxide dismutase (PEG-SOD) to decrease cellular $O_2^{\bullet-}$ and therefore reduce the oxidative stress generated by $ONOO^-$. The extent of the effects of SOD on UVB-induced $[Zn^{2+}]_i$ elevation and apoptosis were determined by the real-time fluorescence measurement and flow cytometry methods as described previously. Our data shows that UVB-induced $[Zn^{2+}]_i$ elevation was totally inhibited by treating the cells with SOD (Fig. 4A). These results suggest that oxidative stress generated from $ONOO^-$ mediates UVB-induced $[Zn^{2+}]_i$ elevation.

Since $ONOO^-$ is considered a highly reactive oxidant and potent inducer of cell death (Szabo et al. 2007), we examined whether treating cells with SOD also reduces UVB-induced apoptosis of the cells. Our data showed that removal of $O_2^{\bullet-}$ reduced apoptotic death of the irradiated cell from 39.1±1.8% to 25.2±1.6% (Fig. 4B). Removal of $O_2^{\bullet-}$ by SOD reduced the apoptotic death of UVB-treated cells by approximately 47% after correcting with the 7−8% of apoptotic cells observed in untreated or SOD alone treated cells. In our previous study, LNAC, the $ONOO^-$ scavenger, was also used to evaluate the effect of peroxynitrite on apoptotic death induced by UVB. Upon LNAC treatment, the UVB-induced apoptotic cell death was reduced 38.6% at 24 h post-irradiation (Wu et al. 2010). These results also indicate that UVB-induced formation of $ONOO^-$ contributes to apoptotic death of UVB-irradiated cells, which agrees with our recent report (Wu et al. 2010).

TPEN uncouples eNOS in a concentration-dependent manner

In disease condition or extracellular stimuli, the increased monomerization of eNOS alters the enzyme function and generates superoxide instead of $NO^{\bullet}$. This monomerization of eNOS is referred to eNOS uncoupling (Yang et al. 2009). Our data showed that while a higher concentration (> 50 μM) of TPEN induced apoptotic death of HaCaT cells, it also prevented further UVB-induced apoptosis of the cells (Fig. 3A). This result suggests that high [TPEN] may share the upstream signaling pathway with UVB in induction of apoptosis (Fig. 6). Previous report indicated that TPEN could uncouple eNOS by removing Zn^{2+} from the enzyme in a cell free system and *E. Coli.* (Li et al. 1999; Zou et al. 2002). Our recent studies suggested that UVB could also uncouple eNOS and increase production of $ONOO^{-}$ (Liu and Wu 2009; Wu et al. 2010). Since uncoupled eNOS produces $O_2^{\bullet -}$ (Huk et al. 1997) that was critical for UVB-induced apoptosis (Fig. 4B), we analyzed the effect of [TPEN] on eNOS uncoupling in HaCaT cells. Our data showed that eNOS dimers were significantly reduced immediately after the treatment of 75 μM TPEN (Fig. 5, Lane 4 vs. 1) and were partially recovered at 2 h post-treatment (Fig. 5A, Lane 5 vs. 4). The eNOS dimers were only slightly reduced after the treatment of 12.5 μM TPEN (Fig. 5A, Lane 2 vs. 1) and were totally recovered at 2 h post-treatment (Fig. 5A, Lane 3 vs. 2). These results indicated that TPEN uncouples eNOS in a concentration-dependent manner. These results suggest that eNOS uncoupling might be the pathway that shared by high [TPEN] or UVB induced apoptosis of keratinocytes.

Discussion

UVB induces a rapid release of $NO^{\bullet}$ and $O_2^{\bullet -}$ in cultured keratinocytes (Aitken et al. 2007). Our recent studies demonstrated that UVB induces an immediate increase of cNOS activity and an immediate elevation of $NO^{\bullet}$ and $ONOO^{-}$ in both cultured cells and skin tissue (Wu et al. 2010). An elevation of intracellular level of $NO^{\bullet}$ has been shown to alter intracellular Zn^{2+} homeostasis (Bernal et al. 2008; Frederickson et al. 2002; St Croix et al. 2002), which plays a role in regulation of UV-induced apoptosis (Leccia et al. 1999; McGowan et al. 1994; Parat et al. 1997). However, it has never been reported that UV-irradiation increases intracellular free Zn^{2+} concentration. Our data shows that UVB-irradiation induced a quick elevation of $[Zn^{2+}]_i$ in both HaCaT and HUVEC cells (Fig. 1 and Fig. 2). However, the $[Zn^{2+}]_i$ elevation was behind an increase $NO^{\bullet}$ and $ONOO^{-}$, which were elevated within 45 sec after UVB (Wu et al. 2010). Our data also showed that UVB-induced $[Zn^{2+}]_i$ elevation was dependent on the increase of cNOS activity (Fig. 1F), which has been shown to be responsible for early production of $NO^{\bullet}$ after UVB-irradiation (Wu et al. 2010). In addition to $NO^{\bullet}$, the generation of $O_2^{\bullet -}$ was also critical for UVB-induced $[Zn^{2+}]_i$ elevation since treating the cells with either LNAC or SOD completely eliminated free zinc release after UVB-irradiation (Fig. 1G and Fig. 4A). Since $NO^{\bullet}$ can rapidly react with $O_2^{\bullet -}$ to form $ONOO^{-}$ (Beckman and Koppenol 1996; Groves 1999), our results suggested that UVB-induced $[Zn^{2+}]_i$ elevation is mediated by $ONOO^{-}$.

Zinc homeostasis has been shown to play a role in regulation of apoptosis of cultured skin cells. While chelation of zinc promotes apoptotic cell death, supplement of zinc protects skin cells from UV-induced DNA-damage and apoptosis (Leccia et al. 1999; McGowan et al. 1994; Parat et al. 1997). Our data showed that while higher concentration of TPEN (>50 μM) induced apoptosis, which agreed with a previous report (Parat et al. 1997), it also prevented further apoptosis induced by UVB (Fig. 3). The protective effect was not dependent on the removal of released intracellular Zn^{2+} from UVB-irradiation since lower concentration of TPEN (<25 μM) could also chelate the Zn^{2+}, but had no effect on cell apoptosis with or without UVB-irradiation (Fig. 3). Interestingly, while PARP cleavage is not affected by 12.5 μM TPEN (Fig. 3B, Lane 3 vs. 1), all PARP is cleaved to 89-kD fragment under 75 μM TPEN treatment (Fig. 3B, Lane 5). However, the total amount of PARP is less in the cells treated with 75 μM TPEN

than the amount in the cells treated with 12.5 μM TPEN or without treatment (Fig. 3B Lanes 5,6 vs. 1–4). This could be due to that TPEN activates a caspase-3 independent apoptotic pathway by reduction of PARP expression as previously reported (Parker et al. 2006; Yun et al. 2003). The preventative effect of TPEN on the further UVB-induced apoptosis is likely due to the uncoupling of eNOS (Fig. 5), which leads to a reduction of $NO^{\bullet}$ production upon UVB-irradiation (Fig. 6). Without an elevation of $NO^{\bullet}$, there would be reduced production of $ONOO^{-}$, which is the cause of UVB-induced apoptosis as we recently reported (Wu et al. 2010). However, it was surprising to observe that TPEN could only partially reduced the dimerized cNOS, even at 75 μM (Fig. 5). With K_d for Zn^{2+} at 2.58×10^{-16} M, 75 μM TPEN could reduce cytosolic Zn^{2+} to a subfemtomole level as previously reported (Colvin et al. 2008). The results suggest that zinc may not be essential for the dimerization of cNOS. However we could not rule out that some Zn-cNOS complexes exist in a conformation in which TPEN could not reach the bound ion.

Conclusion

Our results indicate that UVB-induced accumulation of $ONOO^{-}$ and oxidative stress lead to the eNOS uncoupling, intracellular zinc dyshomeostasis, and cell damage via a complex and dynamic regulation. Based on our findings, we proposed a signaling circuit for UVB-induced cNOS uncoupling, Zn^{2+} release and cell death (Fig. 6). UVB activates cNOS, which generates $NO^{\bullet}$. Meanwhile, UVB also generates $O_2^{\bullet-}$, which reacts rapidly with $NO^{\bullet}$ to from $ONOO^{-}$. The elevated $ONOO^{-}$ oxidizes the Zn^{2+}-thiolate center in cNOS and induces cNOS uncoupling and Zn^{2+} release. The uncoupled cNOS produces more $O_2^{\bullet-}$ and leads to further elevation of $ONOO^{-}$, cNOS uncoupling and $[Zn^{2+}]_i$ elevation. The increased $ONOO^{-}$ also leads to an $NO^{\bullet}/ONOO^{-}$ imbalance and promotes apoptosis.

Supplementary Material

Refer to Web version on PubMed Central for supplementary material.

Abbreviations

ANX5	annexin V
CAG-AM	Calcium Green-1 acetoxymethyl ester
cNOS	constitutive nitric oxide synthase
FITC	fluorescein isothiocyanate
HUVEC	human umbilical vein endothelial
LNAC	N-Acetyl-L-Cysteine
LNMMA	N^{G}-monomethyl-L-Arginine
MEF	murine embryonic fibroblast
NG-DCF	Newport Green-DCF
$NO^{\bullet}$	nitric oxide
$O_2^{\bullet-}$	superoxide
$ONOO^{-}$	peroxynitrite
PBS	phosphate buffered saline
PEG-SOD	polyethylene glycol-conjugated superoxide dismutase
PI	propidium iodide

ROS	reactive oxygen species
TPEN N	N,N',N'-tetrakis (2-pyridylmethyl) ethylenediamine
UVB	ultraviolet B light
$[Zn^{2+}]_i$	intracellular Zn^{2+} concentration

Acknowledgments

We thank Drs. Tadeusz Malinski (Ohio University) and Robert A. Colvin (Ohio University) for their insightful discussions. We thank Mr. Josh K. Ketterman for technical assistance in using the confocal microscope. We thank Mr. Oliver L. Carpenter and Ms. Kimberly S. George for editorial assistance. This work is partially supported by 2R56CA086928 (to S. W.) and 2RO1CA086928 (to S. W.).

References

Aitken GR, Henderson JR, Chang SC, McNeil CJ, Birch-Machin MA. Direct monitoring of UV-induced free radical generation in HaCaT keratinocytes. Clinical and experimental dermatology 2007;32:722–727. [PubMed: 17953641]

Aizenman E, Stout AK, Hartnett KA, Dineley KE, McLaughlin B, Reynolds IJ. Induction of neuronal apoptosis by thiol oxidation: putative role of intracellular zinc release. Journal of Neurochemistry 2000;75:1878–1888. [PubMed: 11032877]

Aravindakumar CT, Ceulemans J, De Ley M. Nitric oxide induces Zn2+ release from metallothionein by destroying zinc-sulphur clusters without concomitant formation of S-nitrosothiol. The Biochemical Journal 1999;344 Pt 1:253–258. [PubMed: 10548558]

Beckman JS, Koppenol WH. Nitric oxide, superoxide, and peroxynitrite: the good, the bad, and ugly. The American Journal Of Physiology 1996;271:C1424–C1437. [PubMed: 8944624]

Bernal PJ, Leelavanichkul K, Bauer E, Cao R, Wilson A, Wasserloos KJ, Watkins SC, Pitt BR, St Croix CM. Nitric-oxide-mediated zinc release contributes to hypoxic regulation of pulmonary vascular tone. Circulation Research 2008;102:1575–1583. [PubMed: 18483408]

Bossy-Wetzel E, Talantova MV, Lee WD, Scholzke MN, Harrop A, Mathews E, Gotz T, Han J, Ellisman MH, Perkins GA, Lipton SA. Crosstalk between nitric oxide and zinc pathways to neuronal cell death involving mitochondrial dysfunction and p38-activated K+ channels. Neuron 2004;41:351–365. [PubMed: 14766175]

Canzoniero LM, Turetsky DM, Choi DW. Measurement of intracellular free zinc concentrations accompanying zinc-induced neuronal death. The Journal Of Neuroscience 1999;19:RC31. [PubMed: 10493776]

Colvin RA, Bush AI, Volitakis I, Fontaine CP, Thomas D, Kikuchi K, Holmes WR. Insights into Zn2+ homeostasis in neurons from experimental and modeling studies. American journal of physiology Cell physiology 2008;294:C726–C742. [PubMed: 18184873]

Cuajungco MP, Lees GJ. Zinc metabolism in the brain: relevance to human neurodegenerative disorders. Neurobiology Of Disease 1997;4:137–169. [PubMed: 9361293]

Deliconstantinos G, Villiotou V, Stavrides JC. Alterations of nitric oxide synthase and xanthine oxidase activities of human keratinocytes by ultraviolet B radiation. Potential role for peroxynitrite in skin inflammation. Biochemical pharmacology 1996a;51:1727–1738. [PubMed: 8687488]

Deliconstantinos G, Villiotou V, Stavrides JC. Increase of particulate nitric oxide synthase activity and peroxynitrite synthesis in UVB-irradiated keratinocyte membranes. The Biochemical Journal 1996b; 320 (Pt 3):997–1003. [PubMed: 9003391]

Di Pietro R, Mariggio MA, Guarnieri S, Sancilio S, Giardinelli A, Di Silvestre S, Consoli A, Zauli G, Pandolfi A. Tumor necrosis factor-related apoptosis-inducing ligand (TRAIL) regulates endothelial nitric oxide synthase (eNOS) activity and its localization within the human vein endothelial cells (HUVEC) in culture. Journal Of Cellular Biochemistry 2006;97:782–794. [PubMed: 16229016]

Frederickson CJ, Cuajungco MP, LaBuda CJ, Suh SW. Nitric oxide causes apparent release of zinc from presynaptic boutons. Neuroscience 2002;115:471–474. [PubMed: 12421613]

Groves JT. Peroxynitrite: reactive, invasive and enigmatic. Current Opinion In Chemical Biology 1999;3:226–235. [PubMed: 10226050]

Ha KN, Chen Y, Cai J, Sternberg P Jr. Increased glutathione synthesis through an ARE-Nrf2-dependent pathway by zinc in the RPE: implication for protection against oxidative stress. Investigative Ophthalmology & Visual Science 2006;47:2709–2715. [PubMed: 16723490]

Huk I, Nanobashvili J, Neumayer C, Punz A, Mueller M, Afkhampour K, Mittlboeck M, Losert U, Polterauer P, Roth E, Patton S, Malinski T. L-arginine treatment alters the kinetics of nitric oxide and superoxide release and reduces ischemia/reperfusion injury in skeletal muscle. Circulation 1997;96:667–675. [PubMed: 9244241]

Leccia MT, Richard MJ, Favier A, Beani JC. Zinc protects against ultraviolet A1-induced DNA damage and apoptosis in cultured human fibroblasts. Biological Trace Element Research 1999;69:177–190. [PubMed: 10468155]

Lee SC, Lee JW, Jung JE, Lee HW, Chun SD, Kang IK, Won YH, Kim YP. Protective role of nitric oxide-mediated inflammatory response against lipid peroxidation in ultraviolet B-irradiated skin. The British Journal Of Dermatology 2000;142:653–659. [PubMed: 10792214]

Li H, Raman CS, Glaser CB, Blasko E, Young TA, Parkinson JF, Whitlow M, Poulos TL. Crystal structures of zinc-free and -bound heme domain of human inducible nitric-oxide synthase. Implications for dimer stability and comparison with endothelial nitric-oxide synthase. The Journal of biological chemistry 1999;274:21276–21284. [PubMed: 10409685]

Liu W, Wu S. The Differential Role of Nitric Oxide Synthases in Ultraviolet Light B-induced Apoptosis. The FASEB Journal 2009:890–895.

Lobner D, Canzoniero LM, Manzerra P, Gottron F, Ying H, Knudson M, Tian M, Dugan LL, Kerchner GA, Sheline CT, Korsmeyer SJ, Choi DW. Zinc-induced neuronal death in cortical neurons. Cellular And Molecular Biologyl (Noisy-le-grand) 2000;46:797–806.

Lu W, Laszlo CF, Miao Z, Chen H, Wu S. The role of nitric oxide synthase in regulation of ultraviolet light-induced phosphorylation of the alpha-subunit of eukaryotic initiation factor 2. J Biol Chem. 2009

McGowan AJ, Fernandes RS, Verhaegen S, Cotter TG. Zinc inhibits UV radiation-induced apoptosis but fails to prevent subsequent cell death. International Journal Of radiation Biology 1994;66:343–349. [PubMed: 7930836]

Pacher P, Beckman JS, Liaudet L. Nitric oxide and peroxynitrite in health and disease. Physiological Reviews 2007;87:315–424. [PubMed: 17237348]

Parat MO, Richard MJ, Pollet S, Hadjur C, Favier A, Beani JC. Zinc and DNA fragmentation in keratinocyte apoptosis: its inhibitory effect in UVB irradiated cells. Journal of photochemistry and photobiology B, Biology 1997;37:101–106.

Parker SH, Parker TA, George KS, Wu S. The roles of translation initiation regulation in ultraviolet light-induced apoptosis. Molecular And Cellular Biochemistry 2006;293:173–181. [PubMed: 16786187]

Powell SR. The antioxidant properties of zinc. The Journal Of Nutrition 2000;130:1447S–1454S. [PubMed: 10801958]

Schindl A, Klosner G, Honigsmann H, Jori G, Calzavara-Pinton PC, Trautinger F. Flow cytometric quantification of UV-induced cell death in a human squamous cell carcinoma-derived cell line: dose and kinetic studies. Journal of photochemistry and photobiology B, Biology 1998;44:97–106.

St Croix CM, Wasserloos KJ, Dineley KE, Reynolds IJ, Levitan ES, Pitt BR. Nitric oxide-induced changes in intracellular zinc homeostasis are mediated by metallothionein/thionein. American Journal Of Physiology Lung Cellular And Molecular Physiology 2002;282:L185–L192. [PubMed: 11792622]

Suh SW, Hamby AM, Gum ET, Shin BS, Won SJ, Sheline CT, Chan PH, Swanson RA. Sequential release of nitric oxide, zinc, and superoxide in hypoglycemic neuronal death. Journal Of Cerebral Blood Flow And Metabolism 2008;28:1697–1706. [PubMed: 18545258]

Szabo C, Ischiropoulos H, Radi R. Peroxynitrite: biochemistry, pathophysiology and development of therapeutics. Nature Reviews Drug Discovery 2007;6:662–680.

Taylor CG, McCutchon TL, Boermans HJ, DiSilvestro RA, Bray TM. Comparison of Zn and vitamin E for protection against hyperoxia-induced lung damage. Free Radical Biology & Medicine 1997;22:543–550. [PubMed: 8981047]

Vallee BL, Falchuk KH. The biochemical basis of zinc physiology. Physiological Reviews 1993;73:79–118. [PubMed: 8419966]

Vermes I, Haanen C, Steffens-Nakken H, Reutelingsperger C. A novel assay for apoptosis. Flow cytometric detection of phosphatidylserine expression on early apoptotic cells using fluorescein labelled Annexin V. Journal Of Immunological Methods 1995;184:39–51. [PubMed: 7622868]

Wu S, Wang L, Jacoby AM, Kasinski K, Kubant R, Malinski T. Ultraviolet B Light-Induced Nitric Oxide/Peroxynitrite Imbalance in Keratinocytes – Implication in Apoptosis and Necrosis. Photochemistry and photobiology. 2010 In Press.

Yamaoka J, Kawana S, Miyachi Y. Nitric oxide inhibits ultraviolet B-induced murine keratinocyte apoptosis by regulating apoptotic signaling cascades. Free Radical Research 2004;38:943–950. [PubMed: 15621712]

Yang YM, Huang A, Kaley G, Sun D. eNOS uncoupling and endothelial dysfunction in aged vessels. American Journal Of Physiology Heart And Circulatory Physiology 2009;297:H1829–H1836. [PubMed: 19767531]

Yun SJ, Lee DJ, Kim MO, Jung B, Kim SO, Sohn NW, Lee EH. Reduction but not cleavage of poly (ADP-ribose) polymerase during stress-mediated cell death in the rat hippocampus. Neuroreport 2003;14:935–939. [PubMed: 12802178]

Zou MH, Shi C, Cohen RA. Oxidation of the zinc-thiolate complex and uncoupling of endothelial nitric oxide synthase by peroxynitrite. The Journal of clinical investigation 2002;109:817–826. [PubMed: 11901190]

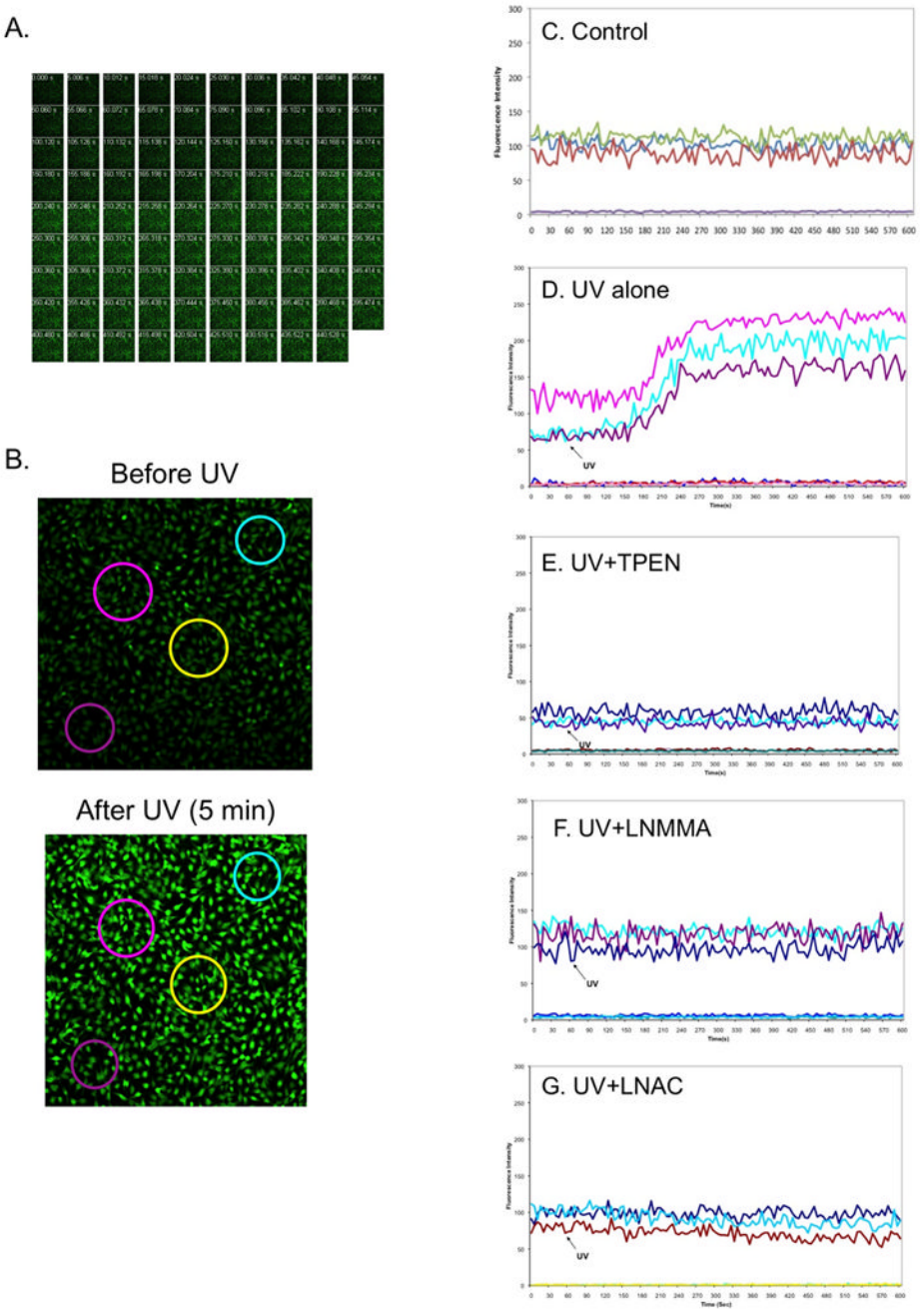

Fig. 1.

NOS activation and oxidative-stress mediate UVB-induced $[Zn^{2+}]_i$ elevation in HaCaT cells. The cells were loaded with NG (10 μM) for 30 min and then the fluorescence of the cells were monitored using a Carl Zeiss confocal microscope. When the background signals of fluorescence were stabilized, the cells were irradiated with UVB (50 mJ/cm^2) and fluorescence intensities at three different areas were continuously recorded. Meanwhile the fluorescence images were captured before and after UVB. Panel A: a series of $[Zn^{2+}]_i$ fluorescence images captured in 5 sec intervals. Panel B: High-resolution pictures of cells captured before and 5 min after UVB-irradiation. Large circles represent individual regions of interests (ROIs) selected for analysis. Panels C–G: Fluorescence intensities were continuously recorded from

the cells that were a control (non-UVB, C), treated by UVB (D), pretreated with 50 μM TPEN (E), 100 μM LNMMA (F) or 25 mM LNAC (G). Individual ROIs were graphed as a function of time. The draw for the first 60 sec was the baseline before cells were irradiated by UVB. Flat lines represent control ROIs drawn in regions free of cells.

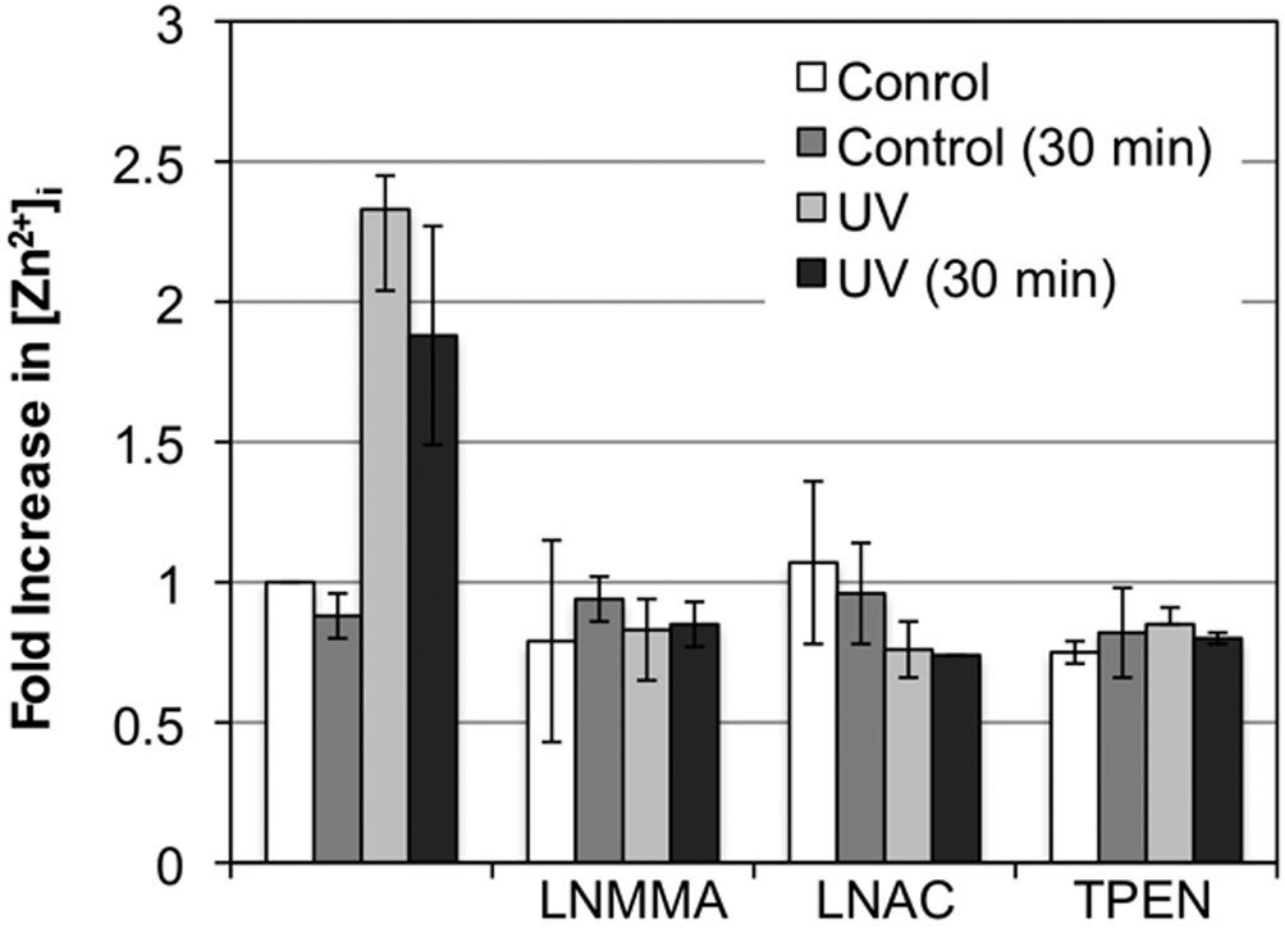

Fig. 2.

NOS activation and oxidative-stress mediate UVB-induced $[Zn^{2+}]_i$ elevation in HUVEC cells. The cells were not treated or treated with LNMMA (100 μM), LNAC (25 mM) and TPEN (50 μM) before loaded with NG for 30 min. The fluorescence intensity was determined using a Spectramax plate reader. Fluorescence intensities were measured immediately and 30 min after UVB irradiated (50 mJ/cm^2) and then normalized to the control group to obtain a ratio for relative $[Zn^{2+}]_i$. The error bars represent the standard deviation of two independent experiments.

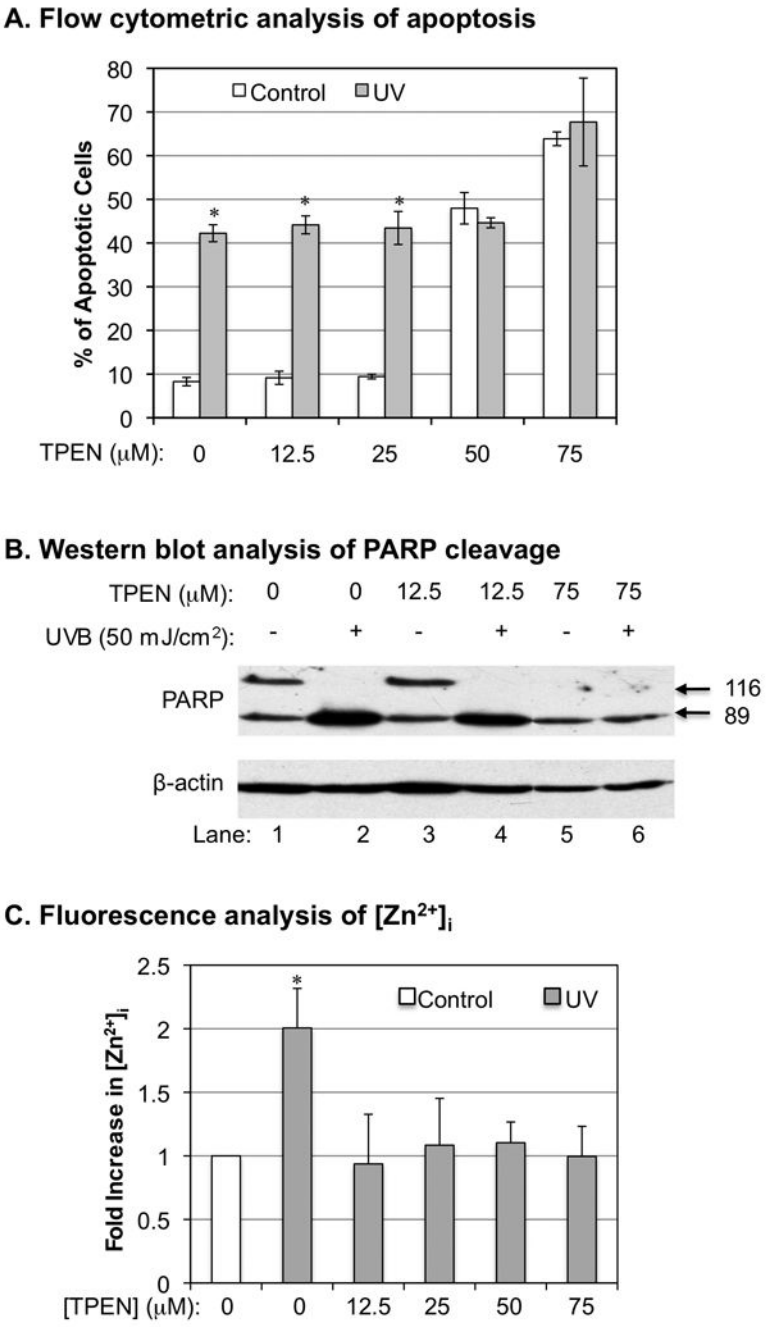

Fig. 3.

The correlations between UVB-induced $[Zn^{2+}]_i$ elevation and apoptosis. HaCat cells were treated with different concentration of TPEN as indicated 15 min before and after UVB-irradiation (50 mJ/cm^2). The amount of Annexin V-FITC and PI double-stained cells were quantitatively analyzed by flow cytometry at 24 h post-irradiation. Panel A: the percentage of Annexin V-FITC/PI positive cells, which represent apoptotic dead cells. The error bars represent the standard deviation of three independent experiments. * $p < 0.05$ vs. UVB alone. Panel B: Western blot analysis of PARP cleavage. Panel C: Relative fluorescence intensities of $[Zn^{2+}]_i$ in UVB or TPEN treated HaCaT cells. The error bars represent the standard deviation of three independent experiments. * $p < 0.05$ vs. UVB alone.

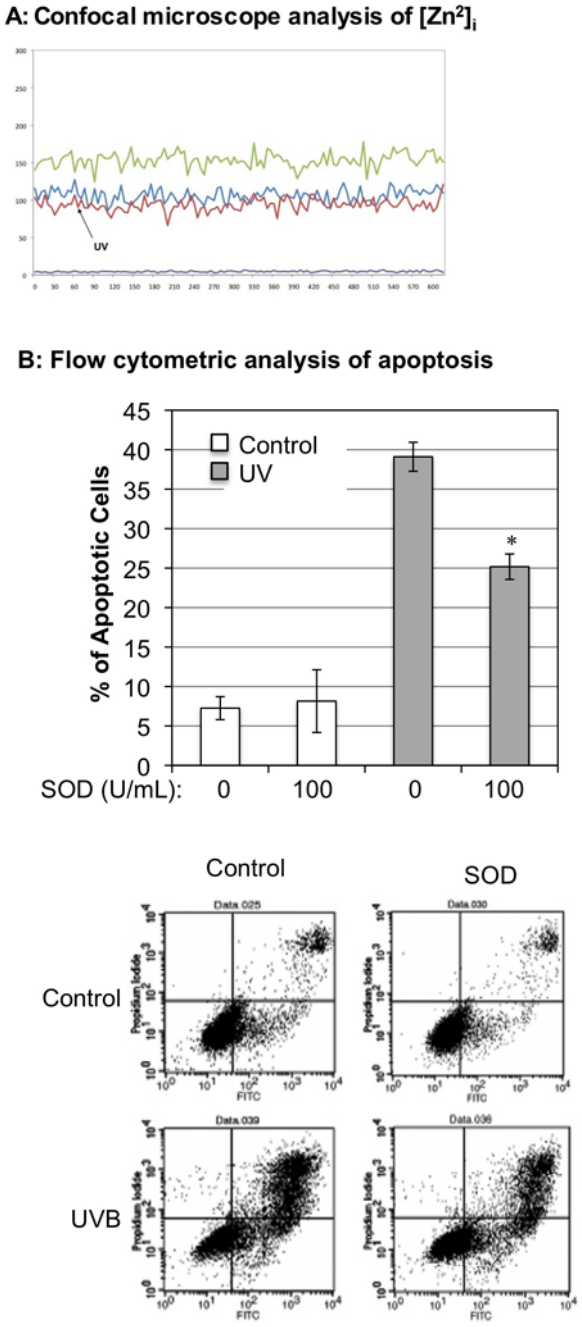

Fig. 4.

Removal of $O_2^{\bullet -}$ prevents $[Zn^{2+}]_i$ elevation and reduces apoptotic cell death after UVB-irradiation. Panel A: NG-DCF fluorescence intensity was recorded from the cells that were treated with PEG-SOD from individual ROIs graphed as a function of time. The background lines represent control ROIs drawn in regions free of the cells. Panel B: The relative percentage of apoptotic cells with or without being pretreated with PEG-SOD after UVB-irradiation (50 mJ/cm^2). The apoptotic cell death was analyzed at 24 h post-irradiation using the Annexin-V/PI double staining and flow cytometry method. The error bars represent the standard deviation of three independent experiments. * $p < 0.05$ vs. UVB alone. The lower panel shows the dot-plot graphs of flow cytometry.

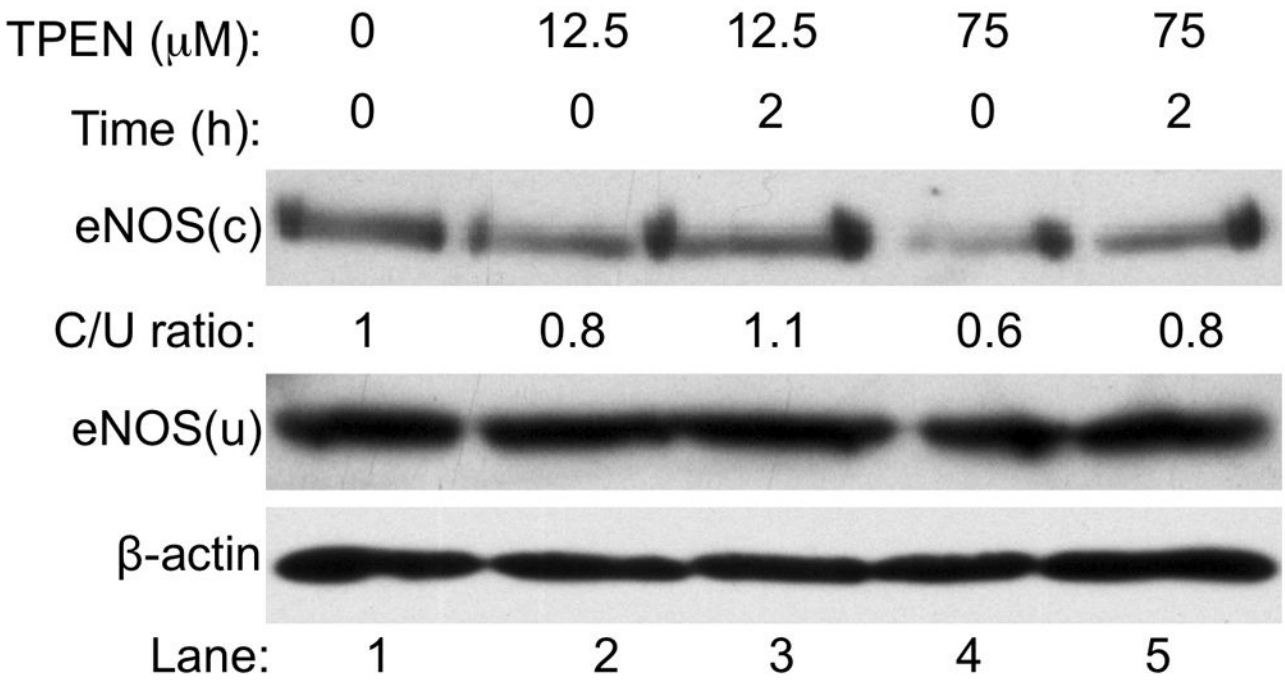

Fig. 5.

The eNOS uncoupling is TPEN concentration-dependent. HaCaT cells were not treated or treated with 12.5 or 75 μM [TPEN] as indicated. Immediately or 2 h after treatment, total lysates were subjected to a low-temperature SDS-PAGE under reducing conditions. The monomer and dimer of eNOS were monitored by Western blot analysis. The intensities of the bands of eNOS were quantitated using ImageJ (v1.42k, NIH) and normalized to the control.

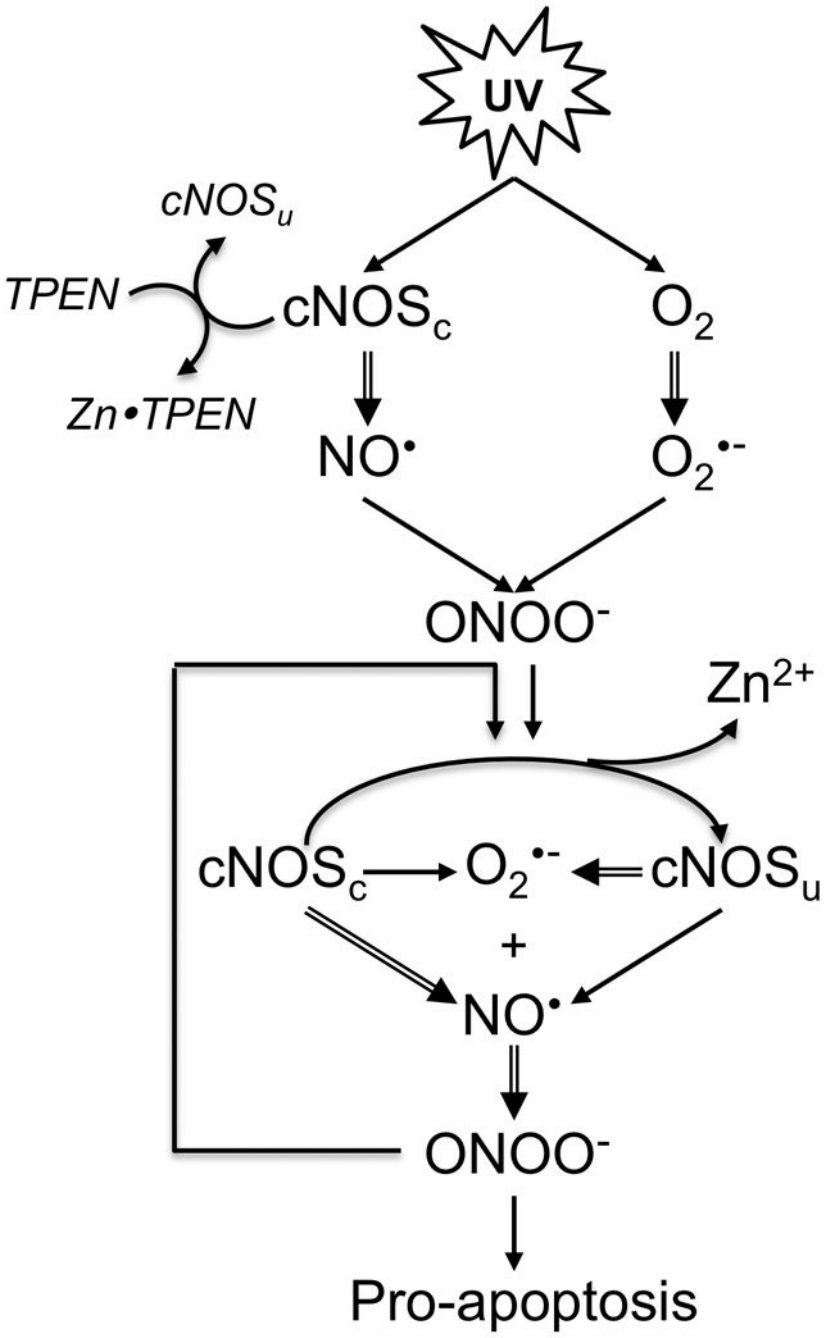

Fig. 6.
Proposed signaling circuits for UVB-induced cNOS uncoupling, Zn^{2+} release and apoptosis. $cNOS_c$: coupled cNOS. $cNOS_u$: uncoupled cNOS.